

Semantics-enhanced Temporal Graph Networks for Content Popularity Prediction

Jianhang Zhu, Rongpeng Li, Xianfu Chen, Shiwen Mao, Jianjun Wu and Zhifeng Zhao

Abstract—The surging demand for high-definition video streaming services and large neural network models (e.g., Generative Pre-trained Transformer, GPT) implies a tremendous explosion of Internet traffic. To mitigate the traffic pressure, architectures with in-network storage have been proposed to cache popular contents at devices in closer proximity to users. Correspondingly, in order to maximize caching utilization, it becomes essential to devise an effective popularity prediction method. In that regard, predicting popularity with dynamic graph neural network (DGNN) models achieve remarkable performance. However, DGNN models still suffer from tackling sparse datasets where most users are inactive. Therefore, we propose a reformative temporal graph network, named semantics-enhanced temporal graph network (STGN), which attaches extra semantic information into the user-content bipartite graph and could better leverage implicit relationships behind the superficial topology structure. On top of that, we customize its temporal and structural learning modules to further boost the prediction performance. Specifically, in order to efficiently aggregate the diversified semantics that a content might possess, we design a user-specific attention (UsAttn) mechanism for temporal learning module. Unlike the attention mechanism that only analyzes the influence of genres on content, UsAttn also considers the attraction of semantic information to a specific user. Meanwhile, as for the structural learning, we introduce the concept of positional encoding into our attention-based graph learning and adopt a semantic positional encoding (SPE) function to facilitate the analysis of content-oriented user-association analysis. Finally, extensive simulations verify the superiority of our STGN models and demonstrate the effectiveness in content caching.

Index Terms—Content caching, popularity prediction, dynamic graph neural network, semantics.

I. INTRODUCTION

THE surging demand for high-definition video streaming services and large neural network models results in a tremendous pressure on the Internet [1]–[3]. It is pointed out that caching popular contents or models in advance has the potential to reduce the backhaul traffic up to 35% [4]. Correspondingly, in-network caching emerges as a promising technique and garners extensive attention [5], [6]. However, compared with the continual explosion of content volume, it

is infeasible to increase the device caching capability immoderately due to the practical limitations (e.g., economic and technical perspectives) [7]. This predicament makes the design of competent caching strategies much more crucial, wherein accurate popularity prediction plays a decisive role [7].

Recently, deep neural networks (DNNs) have demonstrated their remarkable potential by unveiling the embedded temporal correlation for popularity prediction [8]–[10]. Meanwhile, along with users requesting contents, the interactions between users and contents gradually constitute a dynamic bipartite interaction graph. Some recent graph neural network (GNN) model-based methods, which resort to exploiting the inherent structural pattern in such a bipartite graph, manifest themselves in providing superior prediction accuracy within a recommendation system (RS) [11], [12]. In particular, such GNN models enable us to speculate for inactive users with few requests in an interaction-intense graph by associating them with other active users that exhibit similar behaviors. However, these GNN models [11], [12] are contingent on an assumption of a static bipartite graph. In order to blend the merits of both structural learning and temporal learning, recommendation with dynamic graph neural network (DGNN) models emerges [13], which is always synergistic with caching [14]. Thus, caching with DGNN models also achieves satisfactory improvement [15].

Nevertheless, Ref. [15] discovers that the model’s performance is not gratifying for cases where most users in the bipartite graph are inactive. To overcome the data sparsity, enlarging the receptive field of the DGNN model (e.g., the stacking of GNN layers or an increase in the number of first-order neighbors) might be productive [16], but it incurs significant computational complexity and time cost as well. On the contrary, along with fine-grained methods, enlarging the breadth of available information, such as considering the side information of users and contents in DGNN, sounds more appealing [17], [18]. Besides, the side information enriches the sparse graph and may also reflect user’s intention, both of which would benefit the reasoning and interpretability of user’s future behavior. But given the importance of user privacy, it is more appropriate to conduct an excavation for the general content information (e.g., analyzing the semantic correlations among the genre information of contents).

Fig. 1 presents an example of the dynamic interaction graph and the implicit semantic relationship between contents. The requests of two users, u_1 and u_2 , only intersect at content i_3 . The sparsity of data makes it intractable for classical GNN-based methods to accurately predict the preference of u_1 for content i_4 . On the other hand, the content genre information and their underlying similarities in the semantic sphere, which

Jianhang Zhu and Rongpeng Li are with the College of Information Science and Electronic Engineering, Zhejiang University, Hangzhou 310027, China (e-mail: {zhujh20; lirongpeng}@zju.edu.cn).

Xianfu Chen is with VTT Technical Research Centre of Finland, 90570 Oulu, Finland (e-mail: xianfu.chen@vtt.fi).

Shiwen Mao is with Department of Electrical and Computer Engineering, Auburn University, Auburn, AL 36849-5201, USA (email: smao@ieee.org).

Jianjun Wu is with Huawei Technologies Company, Ltd., Shanghai 201206, China (e-mail: wujianjun@huawei.com).

Zhifeng Zhao is with Zhejiang Lab, Hangzhou, China as well as the College of Information Science and Electronic Engineering, Zhejiang University, Hangzhou 310027, China (e-mail: zhaozf@zhejianglab.com).

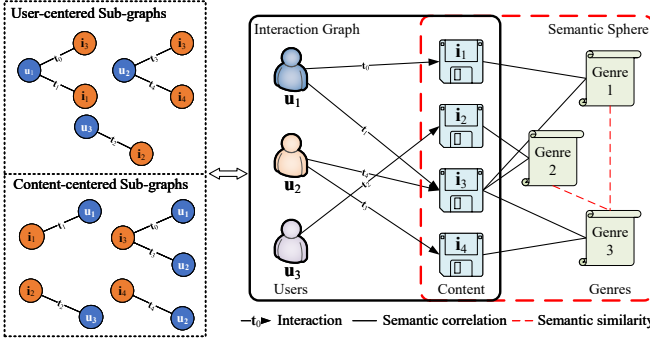


Fig. 1. An example of the dynamic interaction graph and the implicit semantic relationship between contents.

are indicated by the red dotted lines in Fig. 1, reveal a strong correlation between i_4 and i_3 as well as a weak correlation between i_4 and i_1 . Thanks to the attachment of semantics, these two kinds of underlying connectivity between i_4 and i_1 are unveiled to assist the prediction, and an inference that u_1 is likely to request i_4 can be boldly triggered. Furthermore, as demonstrated in Fig. 2, there exist several natural language processing (NLP) methods, such as one-hot, BERT [19], and Glove [20], available for computing the semantic similarities. It is also natural to conjecture that a more precise computation of semantic similarities benefit to a superior speculation.

In this paper, we propose a semantics-enhanced temporal graph network (STGN) to strengthen the DGNN model performance in dealing with sparse datasets and realize the semantics-assisted popularity prediction in content caching task. In particular, semantics ameliorates the temporal learning module to better track the dynamical variations in a user-content bipartite graph, and circumvents the difficulties in discovering patterns in the sparse dataset attributed to the supplement to content-centered sub-graphs for the structural learning. Besides, we adopt some mature NLP methods to encode genre messages as semantic information, and then treat the embedded semantic information as part of the input of the predictive model. Additionally, considering that a content might possess multiple genres (e.g., a fictional action movie containing both fiction and action genres) and the predilection might vary across users as well, we further design a user-specific attention (UsAttn) mechanism for a more fine-grained aggregation of various semantics, so as to improve the utilization of the diversified semantic features. Unlike the attention mechanism that only considers the influence of genres in content, UsAttn leverages user-content pairs in the bipartite graph and capably analyzes the attraction of semantic information to a specific user during the prediction. Meanwhile, given the massive relevancy among users to the same content and the complication to distinguish one specific user from a content-centered sub-graph, as shown in Fig. 1, the aforementioned enhancement in UsAttn cannot be applied into the semantic analysis in our attention-based structural learning module. Instead, it requires some modification from some fresh perspective. Specifically, inspired by the preliminary effectiveness of a dot-product-based positional encoding (PE) function in Transformer [21], we develop a semantic positional encoding function (SPE), deduced from

TABLE I
MAJOR NOTATIONS USED IN THE PAPER.

Notation	Definition
u_j, i_k	User j and content k
\mathcal{U}, \mathcal{I}	The sets of users and contents
$\mathbf{v}_{u_j}, \mathbf{v}_{i_k}, \mathbf{e}_{jk}$	Raw features of u_j, i_k and their edges
$\mathcal{V}_{\mathcal{U}}, \mathcal{V}_{\mathcal{I}}, \mathcal{E}$	The raw feature sets of users, contents and their edge
$p_{jk}(\hat{T})$	Real preferences of u_j for i_k at \hat{T}
$\tilde{p}_{jk}(\hat{T})$	Predicted preferences of u_j for i_k at \hat{T}
p_{thre}	Threshold value for judging
$\text{Pop}^{i_k}(\hat{T})$	Popularity of i_k at \hat{T}
$\mathbb{P}^{i_k}(\Delta_P)$	Popularity of i_k during the cache updating period Δ_P
δ_p	Popularity predicting period
K	Maximum number of caching capability
$\mathcal{C}(\Delta_P)$	Real request set during the update period
$\tilde{\mathcal{C}}(\Delta_P)$	Predicted popularity set for all contents during Δ_P
$\tilde{\mathcal{C}}_K(\Delta_P)$	Caching set during Δ_P
$h(\Delta_P)$	Cache hit rate
\mathbf{Msg}_{jk}	Message that merges all raw features of an interaction
\mathbf{Msg}_{jk}^s	The semantics-enhanced message
$\mathbf{h}_j(\hat{T})$	Short-term preference of u_j
\mathbf{Mem}_j	Long-term preference of u_j
\mathbf{Mem}_j'	The updated long-term preference of u_j concatenated with extra features
$\mathbf{E}_{u_j}(\hat{T}), \mathbf{E}_{i_k}(\hat{T})$	Final embedding representations for u_j and i_k
\mathbf{E}_{jk}	User-specific embedding
s_{kN_s}	The N_s -th semantic information of i_k
S_{jk}	User-specific semantic feature for u_j and i_k
S_k	Aggregated semantic feature for i_k

a Fourier kernel-based method, to improve the effectiveness of incorporating multi-dimensional semantics in structural learning. Furthermore, we apply our proposed model to a caching strategy in a multi-tier caching system and conduct extensive simulations to evaluate its superiority. Overall, the main contributions of this paper are summarized as follows.

- To deal with the data sparsity, we propose an STGN to leverage the implicit connections between requested contents and their semantic features from both temporal and structural learning perspectives.
- Motivated by the fact that a content usually carries various semantic information, we devise a UsAttn mechanism to exploit potential semantic correlations within the user-content bipartite graph and strengthen the temporal learning.
- In order to improve the effectiveness of semantics in structural learning, we incorporate a theoretical-grounded multi-dimensional SPE, derived from Fourier kernel, into the attention-based graph learning module.
- Extensive experiments based on a real-world dataset verify the improvement in prediction performance achieved by our STGN model and validate the effectiveness of the STGN model-based proactive caching strategy in terms of the cache hit rate.

The remainder of this paper is organized as follows. The related works are discussed in Section II. Then, we introduce system models and formulate the problem in Section III. We elaborate on the details of the main contributions, the proposed prediction model and its modified versions for effective semantic learning in Section IV and V. In Section VI, we present the experimental results and discussions. Finally, the

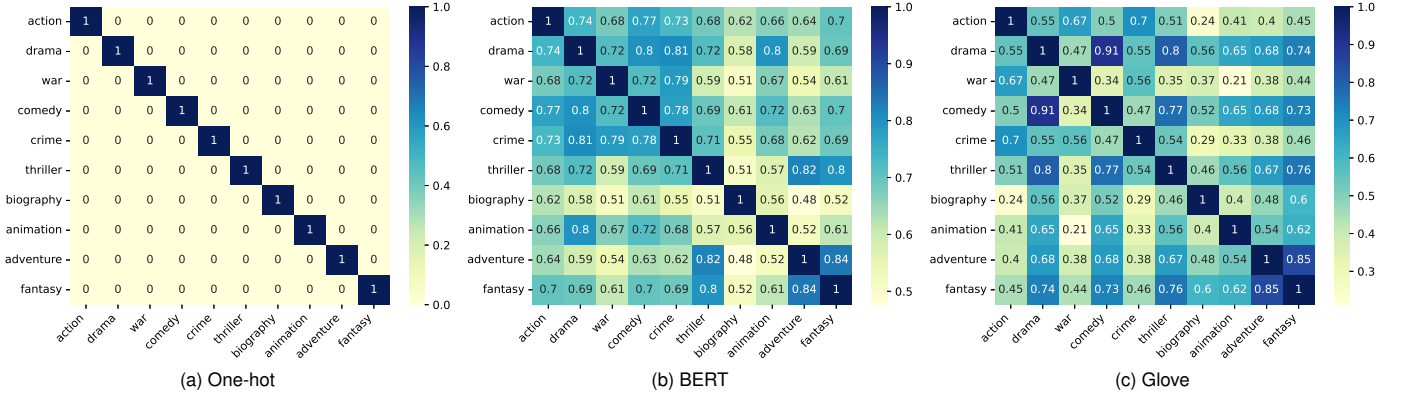


Fig. 2. The visualization of cosine similarities between some genres’ embeddings computed by different NLP methods.

conclusion is summarized in Section VII.

For convenience, we also list the mainly used notations of this paper in Table I.

II. RELATED WORK

Traditionally, albeit the remarkable portability, the widely-mentioned reactive caching strategies, such as least recently used (LRU) and least frequently used (LFU), only focus on the patterns of local requests, thus failing to handle the unexpected requests [22]. Accordingly, it becomes inevitable to design proactive caching strategies, wherein accurate popularity prediction plays a decisive role [7]. With the development of artificial intelligence (AI), applying DNN to predict popularity has thrived. For instance, in [8], a model based on stacked autoencoders (SAE) is proposed to compute the popularity from the content request sequence. In addition, Refs. [9], [10] use a recurrent neural network (RNN) and its variant LSTM to discover the patterns within the temporal content requests, so as to facilitate popularity-assisted content caching. Nevertheless, due to the insufficient historical data, LSTM or other sequence-based prediction models may fail to predict accurately for those inactive users.

Furthermore, the user-content interactions constitute a bipartite graph and lay the very foundation for adopting GNN to enhance the learning performance [12]. Although GNN has won remarkable achievement in RS [11], most existing works assume that the underlying graph is static, which does not conform to the real-life [13]. Consequently, popularity prediction with DGNN has been attracting significant attention. Different from the conventional GNN, a DGNN model is able to jointly learn the structural and temporal patterns of dynamic graphs. For example, Ref. [23] proposes a DyRep model to calculate the dynamic graph with a recurrent architecture. Learning from the “positional encoding” of the self-attention mechanism in Transformer [21], Ref. [16] proposes a “time encoding function” to encode the timestamp information for the graph attention network (GAT) [24], which is called the temporal graph attention mechanism (TGAT). TGN in [25] introduces an additional temporal learning module on top of the TGAT for a deeper refinement of the temporal characteristics. Ref. [15] optimizes the temporal learning module of TGN with an age of information (AoI) based attention mechanism to filter and aggregate fresh historical messages, and realizes satisfactory

results in content caching. Nevertheless, when most users in the graph are inactive, it is in general difficult to obtain satisfactory caching performance by deploying existing DGNN models in a straightforward way.

To overcome the challenge due to the data sparsity, Ref. [16] suggests that it is beneficial to stack more TGAT layers for enlarging the receptive field, but it comes at the expense of massive computation cost. On the other hand, some works attempt to solve this problem by supplementing the side information of the bipartite graph (e.g., user social influence [17]). Refs. [18], [26]–[29] propose to introduce a knowledge graph (KG) for incorporating the side information of the requested contents into a static graph model, which leverages the implicit associations among the contents and yields superior prediction performance. However, these works ignore the dynamics of the interaction graph, while the KG construction also implies the demand for a significant amount of side information (e.g., the director and release date of the content), which may not be available in many cases. Therefore, it is more worthwhile to leverage limited content information (e.g., genre information) with a deeper excavation. In that regard, the astonishing development of NLP, such as one-hot, BERT [19], and GloVe [20], makes it promising to capture the implicit semantic relations between the words.

Meanwhile, it is meaningful to develop effective means of computing embeddings, so as to better unveil correlations. As for the temporal learning, it is simple and sufficient to adopt a $UsAttn$ -based mechanism to discover the relationship between multiple genres related to contents and users. However, it becomes troublesome for the structural learning module, considering the massive relevance among users to the same content. The illuminated work in Ref. [16], which generalizes the definition of position and encodes the timestamps with a customized PE function, motivates us to treat the semantic information as a special kind of position. Therefore, we adopt an SPE to strengthen the association analysis between two semantics-attached content embeddings. As a specially designed PE function, it is also inspired by works with learnable approaches to encode positions [19], [30]. Besides, considering the heavy computational cost and non-uniform decay in different dimensions to encode each dimension independently before the concatenation [31], [32], in SPE , we treat the multi-dimensional position as a whole and

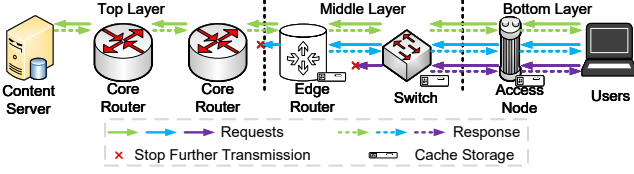


Fig. 3. Caching and response in a multi-tier caching system.

encode it directly by learnable Fourier features [31]. To our best knowledge, the proposed SPE belongs to the first work to view the multi-dimensional semantic information as the position and encode from the perspective of Fourier features.

III. SYSTEM MODELS AND PROBLEM FORMULATION

A. System Models

1) Network Model

As shown in Fig. 3, we concentrate on a multi-tier caching system, where caches are scattered over the devices close to users, such as the *edge routers*, *switches*, and some *access equipment*. We conceptually simplify the network as a three-layer topology as below.

- *Top Layer* – It is composed of *core routers*, which are responsible for connecting content providers with other network elements.
- *Middle Layer* – It encompasses *edge routers* and *switches*. In particular, the *switches* usually connect various devices in a network and communicate with the core network through the *edge routers*. And the location of *switches* is lower than the *edge routers*, while they are in the same layer.
- *Bottom Layer* – It consists of *access equipment*, which are deployed to connect users with the *switches*.

In this paper, we primarily take account of the in-network caching capability of the *access equipment*, *switch*, and *edge router*, and denote them as *Tier 1*, *Tier 2*, and *Tier 3*, respectively. Moreover, as depicted in Fig. 3, once a copy of the target content is cached at a lower-tier device, the request will be directly responded and no longer be sent to any higher-tier devices.

2) Request Model

In this paper, we model the request records in the format of user-content pairs as a graph. We denote the set of users as $\mathcal{U} = \{u_0, u_1, \dots, u_j\}$ and the set of contents as $\mathcal{I} = \{i_0, i_1, \dots, i_k\}$, where u_j and i_k denote the user j and content k , respectively. Furthermore, we allocate raw features for the sets of users and contents with a random initialization method, which are deemed as the input of the predictive model. The raw feature sets of users and contents are denoted as $\mathcal{V}_{\mathcal{U}} = \{\mathbf{v}_{u_0}, \mathbf{v}_{u_1}, \dots, \mathbf{v}_{u_j}\}$ and $\mathcal{V}_{\mathcal{I}} = \{\mathbf{v}_{i_0}, \mathbf{v}_{i_1}, \dots, \mathbf{v}_{i_k}\}$, where \mathbf{v}_{u_j} and \mathbf{v}_{i_k} are the vertexes in the dynamic bipartite graph corresponding to u_j and i_k , respectively. The interactions, i.e., users requesting contents, can be naturally regarded as the edges, which can be denoted as $\mathcal{E} = \{\mathbf{e}_{00}, \mathbf{e}_{01}, \dots, \mathbf{e}_{jk}\}$. Herein, \mathbf{e}_{jk} represents the vector of interactions between u_j and i_k , and reflects the user-behavior type (e.g., watching videos or listening to music).

Next, we formulate the the evolving interactions as a dynamic graph using a set of quadruples, $\mathcal{G} = \{(\mathbf{v}_{u_0}, \mathbf{v}_{i_0}, \mathbf{e}_{00}, T_0), \dots, (\mathbf{v}_{u_j}, \mathbf{v}_{i_k}, \mathbf{e}_{jk}, T_n)\}$, where T_n denotes the timestamp of the n -th interaction¹. In addition, we integrate each quadruple into a piece of historical message as the input of our DGNN model. For instance, the interaction occurred at T_n between u_j and i_k is formulated as $\mathbf{Msg}_{jk} = [\mathbf{v}_{u_j} || \mathbf{v}_{i_k} || \mathbf{e}_{jk} || T_n]$, where $||$ is the concatenation operator. Moreover, as presented before, content may contain various semantic genres, and we need to encode all N_s genres of content i_k with the NLP methods for fully utilizing the inherent semantic characteristics in the subsequent prediction. Correspondingly, the encoded semantic features are represented as $\mathcal{S}_k = \{\mathbf{s}_{k1}, \dots, \mathbf{s}_{kN_s}\}$.

B. Problem Formulation

In this paper, we evaluate the performance of our STGN model in the caching task with cache hit rate. Considering the existence of a maximum number of caching items K , only the top- K contents $\tilde{\mathcal{C}}_K(\Delta_P)$ in a popularity ranking list $\tilde{\mathcal{C}}(\Delta_P)$ are cached during the cache updating period Δ_P . Given the real request set is $\mathcal{C}(\Delta_P)$, we calculate the hit rate during the cache updating period Δ_P with

$$h(\Delta_P) = \frac{\mathbf{I}(\mathcal{C}(\Delta_P), \tilde{\mathcal{C}}_K(\Delta_P))}{\mathbf{I}(\mathcal{C}(\Delta_P), \mathcal{C}(\Delta_P))}, \quad (1)$$

where $\mathbf{I}(\mathcal{X}, \mathcal{Y})$ represents the hit number for the element in \mathcal{Y} to \mathcal{X} .

In line with the previous analysis, to maximize cache hit rate $h(\Delta_P)$, the more popular contents should be cached at the devices closer to the users [33]. Therefore, it becomes essential to know the popularity of each content and obtain the popularity ranking list $\tilde{\mathcal{C}}(\Delta_P)$ in advance. We assume the list is sorted based on the popularity combining outcomes from several time slots $\delta_p \ll \Delta_P$. Therefore, the overall popularity of i_k during the update period Δ_P can be formulated as

$$\mathbb{P}^{i_k}(\Delta_P) = \sum_{n_\delta \in N_\delta} \text{Pop}^{i_k}(n_\delta \times \delta_p), \quad \forall i_k \in \mathcal{I}, \quad (2)$$

where $N_\delta = \{0, 1, \dots, \lfloor \frac{\Delta_P}{\delta_p} \rfloor\}$, $\lfloor \cdot \rfloor$ is a floor operator, and $\text{Pop}^{i_k}(\hat{T})$ represents the popularity of i_k at the future time $\hat{T} = n_\delta \times \delta_p$. Consequently, the popularity ranking list can be obtained to guide the content caching task. Notably, in order to distinguish the contents with the same popularity, we decide their prioritization consistent with LRU.

Obviously, the popularity $\text{Pop}^{i_k}(\hat{T})$ is indispensable, and it can be obtained by gathering the preferences of all users [34], which we calculate as

$$\text{Pop}^{i_k}(\hat{T}) = \sum_j \mathbf{1}(p_{jk}(\hat{T}) > p_{\text{thre}}), \quad \forall i_k \in \mathcal{I}, \quad (3)$$

where $p_{jk}(\hat{T})$ indicates the real preference of u_j for i_k at \hat{T} , p_{thre} is the threshold value for judging emergence of such a request, and $\mathbf{1}(\zeta)$ is an indicator function that only equals 1 if the condition ζ is satisfied.

¹Notably, for simplicity of representation, we omit the superscript j and k of the vertexes T_n^{jk} , which represents the n -th interaction that happens between u_j and i_k .

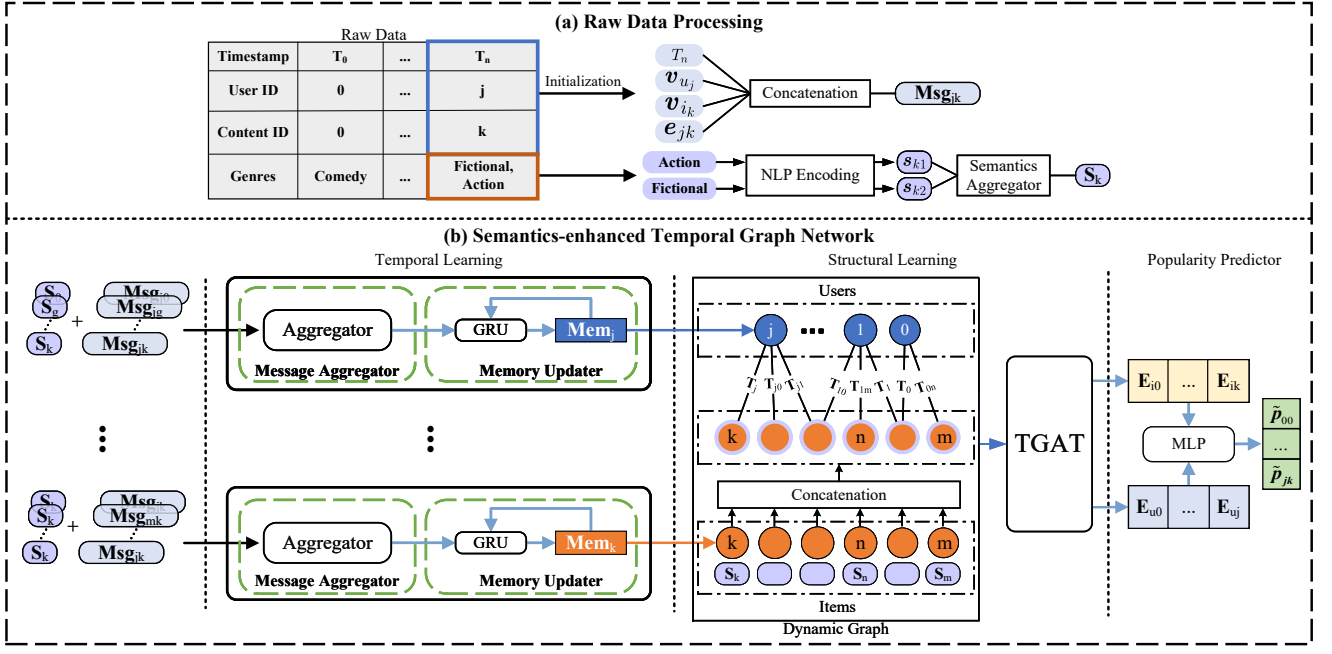


Fig. 4. An illustration of M2-STGN, a TGN model enhanced with semantics in both temporal and structural learning.

As real preference p_{jk}^2 is unknown apriori, we aim to calculate a predicted result \tilde{p}_{jk} with the embeddings of u_j and i_k at \hat{T} , namely $\mathbf{E}_{u_j}(\hat{T})$ and $\mathbf{E}_{i_k}(\hat{T})$. That is,

$$\tilde{p}_{jk}(\hat{T}) = F(\mathbf{E}_{u_j}(\hat{T}), \mathbf{E}_{i_k}(\hat{T})), \quad (4)$$

where a multi-layer perceptron (MLP) can be adopted to realize the function $F(\cdot)$. In this regard, our target in (1) converts to generating feasible representations with the predictive model from the dynamic interaction graph, so as to minimize the binary cross entropy loss (BCELoss) between the real preference, p_{jk} , and the predicted one, \tilde{p}_{jk} , $\forall u_j \in \mathcal{U}$, $i_k \in \mathcal{I}$,

$$\mathcal{L} = - \sum_{u_j, i_k} (p_{jk} \log(\tilde{p}_{jk}) + (1 - p_{jk}) \log(1 - \tilde{p}_{jk})). \quad (5)$$

IV. SEMANTICS-ENHANCED TEMPORAL GRAPH NETWORK

In this section, we focus on the design of the STGN, so as to obtain the desired embedding representations, $\mathbf{E}_{u_j}(\hat{T})$ and $\mathbf{E}_{i_k}(\hat{T})$, $\forall u_j \in \mathcal{U}$, $i_k \in \mathcal{I}$, from a sparse dataset.

A. The Conventional TGN

According to the different roles in prediction, the conventional TGN model is come down to two prime segments, including the temporal learning module and the structural learning module.

1) Temporal Learning Module

The temporal learning module, which consists of a message aggregator and a memory updater, is adopted to compress a user's historical messages into a refined representation. Specifically, the message aggregator leverages several fresh historical messages of u_j before the prediction time \hat{T} to

obtain a compressed feature $\mathbf{h}_j(\hat{T})$. Thus, $\mathbf{h}_j(\hat{T})$ can also be deemed as a feature that is able to represent the short-term preference of u_j , which can be formulated as

$$\mathbf{h}_j(\hat{T}) = \text{Agg}(\mathbf{Msg}_{j,0}, \dots, \mathbf{Msg}_{j,k}), \quad (6)$$

where $\text{Agg}(\cdot)$ is a filtering and aggregation function that can be implemented diversely. In the remainder of this paper, we primarily consider three approaches, including filtering the latest message, using the mean value of all messages [25], and an attention-based weighted summation of limited fresh messages with an AoI filter [15]. We denote them as TGN-L, TGN-M, and TGN-A, respectively.

Subsequently, in order to acquire a much more representative temporal feature, a memory updater is adopted to update the long-term preference \mathbf{Mem}_j based on the compressed short-term preference $\mathbf{h}_j(\hat{T})$. In order to realize the updater, a learnable function, such as LSTM or the gated recurrent unit (GRU), is necessary. Here, considering the advantage in convergence speed [35], we complete the update procedure with a GRU, which is mathematically formulated as

$$\begin{aligned} \mathbf{Mem}_j &\leftarrow \mathbf{Z} \cdot \mathbf{H} + (1 - \mathbf{Z}) \cdot \mathbf{Mem}_j, \\ \mathbf{Z} &= \sigma(\mathbf{h}_j(\hat{T})\mathbf{W}_{hZ} + \mathbf{Mem}_j\mathbf{W}_{MZ} + \mathbf{b}_Z), \\ \mathbf{H} &= \tanh(\mathbf{h}_j(\hat{T})\mathbf{W}_{hH} + (\mathbf{F} \cdot \mathbf{Mem}_j)\mathbf{W}_{MH} + \mathbf{b}_H), \\ \mathbf{F} &= \sigma(\mathbf{h}_j(\hat{T})\mathbf{W}_{hF} + \mathbf{Mem}_j\mathbf{W}_{MF} + \mathbf{b}_F), \end{aligned} \quad (7)$$

where \mathbf{W}_{hZ} , \mathbf{W}_{hF} , \mathbf{W}_{hH} , \mathbf{W}_{MZ} , \mathbf{W}_{MF} and \mathbf{W}_{MH} denote the trainable weights, while \mathbf{b}_Z , \mathbf{b}_F and \mathbf{b}_H are the learnable bias values of the GRU. $\sigma(\cdot)$ and $\tanh(\cdot)$ are the activation functions.

2) Structural Learning Module

The structural learning module aims to generate embeddings for future prediction. Especially, it is also responsible for keeping the representations of the inactive users up-to-date by

²Notably, for simplicity of representation, we omit the \hat{T} of the $p_{jk}(\hat{T})$, $\tilde{p}_{jk}(\hat{T})$, the embeddings $\mathbf{E}_{u_j}(\hat{T})$ and $\mathbf{E}_{i_k}(\hat{T})$ in the following equations.

exchanging features among neighbors in the graph. Obviously, the timestamp of each interaction also plays a vital role in the mapping procedure. Therefore, we adopt a TGAT model [16] to accomplish this unconventional structural learning. Notably, the TGAT mechanism is a module that deploys a learnable time encoding function on the basis of a classical GAT module [24]. In particular, the specially designed time encoding function is formulated as

$$\Phi_{d_T}(\Delta_t) = \sqrt{\frac{1}{d_T}} [\cos(\omega_1 \Delta_t), \dots, \cos(\omega_{d_T} \Delta_t)]^T, \quad (8)$$

where $\omega_1, \omega_2, \dots$ and ω_{d_T} are the trainable parameters, Δ_t denotes the time slot between the interaction-occurring time T_n and the time to predict \hat{T} , (i.e., $\Delta_t = \hat{T} - T_n$). d_T is the dimension number of the desired time encoding.

Then, the encoded time features are concatenated to the output of the temporal learning module \mathbf{Mem}_j as the input for the structural learning.

$$\mathbf{Mem}'_j = [\mathbf{Mem}_j || \Phi_{d_T}(0)], \quad (9)$$

where (9) supplements the updated long-term preference \mathbf{Mem}'_j of u_j with the time feature. It is noteworthy that u_j is the center node of a user-centered sub-graph that we want to learn, so we define $\Delta_t = 0$ for its prediction. As for u_j 's neighbor $k \in \mathcal{N}_j$, its modified preference term \mathbf{Mem}'_k is formulated as

$$\mathbf{Mem}'_k = [\mathbf{Mem}_k || \Phi_{d_T}(\Delta_{t_k})], \forall k \in \mathcal{N}_j, \quad (10)$$

Notably, \mathbf{Mem}'_j and \mathbf{Mem}'_k are the inputs for the structural learning module. As depicted in Fig. 4, the GAT architecture [24] is the paramount part of a TGAT layer to achieve the structural learning of u_j 's dynamic sub-graph, and it can be encapsulated as

$$\mathbf{E}_{u_j}(\hat{T}) = \text{GAT}(\mathbf{Mem}'_j, \mathbf{Mem}'_{\mathcal{N}_j}), \quad (11)$$

Similarly, we can generate the embedding $\mathbf{E}_{i_k}(\hat{T})$ from the content-centered sub-graph of i_k with

$$\begin{aligned} \mathbf{Mem}'_k &= [\mathbf{Mem}_k || \Phi_{d_T}(0)], \\ \mathbf{Mem}'_j &= [\mathbf{Mem}_j || \Phi_{d_T}(\Delta_{t_j})], \forall j \in \mathcal{N}_k, \\ \mathbf{E}_{i_k}(\hat{T}) &= \text{GAT}(\mathbf{Mem}'_k, \mathbf{Mem}'_{\mathcal{N}_k}), \end{aligned} \quad (12)$$

Note that $\mathbf{E}_{u_j}(\hat{T})$ and $\mathbf{E}_{i_k}(\hat{T})$ are utilized as the input of the prediction module in (4). Furthermore, the stacking of multiple TGAT layers can leverage more hidden information within the graph by aggregating multi-hop neighbors. But the enlargement of receptive field also implies greater computational complexity [16]. Thus, we only investigate the performance with a one-layer TGAT to shorten the training session in our simulations.

B. Semantic Enhancement for TGN

Essentially, the temporal learning module in TGN can be deemed as a procedure for refining the commonality from the temporal perspective. However, the randomly initialized raw features make it complicated to accurately extract and analyze the patterns, especially for a sparse dataset. Consequently,

we resort to supplementing the raw input with semantic information, so as to improve the abilities of reasoning and interpretability of our model by extracting the implicit semantic correlations among the contents.

We use some pre-trained NLP models, such as one-hot, BERT [19], and Glove [20], to encode the content genre information as semantic messages, $\mathcal{S}_k = \{s_{k1}, \dots, s_{kN_s}\}$. For the sake of simplicity, we adopt the summation as a semantic aggregator to generate the aggregated feature \mathbf{S}_k from \mathcal{S}_k , which is then incorporated into the raw message as shown in Fig. 4(b). In specific,

$$\mathbf{S}_k = \sum_{n \in N_s} \sigma(\mathbf{W}_s s_{kn} + \mathbf{b}_s), \quad (13)$$

$$\mathbf{Msg}'_{jk} = \sigma(\mathbf{W}_1^t \mathbf{Msg}_{jk} + \mathbf{W}_2^t \mathbf{S}_k), \quad (14)$$

where $\mathbf{W}_s, \mathbf{b}_s, \mathbf{W}_1^t$ and \mathbf{W}_2^t are the trainable parameters to enhance the semantic features, while \mathbf{Msg}'_{jk} is the desired semantics-enhanced historical message in (6). As \mathbf{Msg}'_{jk} can be directly applied to enhance the temporal learning by replacing \mathbf{Msg}_{jk} in (6), we regard such an approach as the semantics-enhanced TGN in a temporal manner, and denote it as M1-STGN.

As we discussed above, although the fresh features for inactive users can be located with the help of the graph structure, the performance still suffers from data sparsity. To address this issue, we further attach the semantic features to the input of the structural learning module, establishing implicit semantic pathways for the dynamic graph from the semantic sphere. In our experiments, we also discover that concatenation outperforms summation for merging semantics in the structural learning module. Then, (10) is further modified as

$$\mathbf{Mem}'_k = [\mathbf{Mem}_k || \mathbf{S}_k || \Phi_{d_T}(\Delta_{t_k})], \forall k \in \mathcal{N}_j, \quad (15)$$

where \mathbf{S}_k is calculated by (13) as well. Similarly, we use M2-STGN to represent the TGN model that is further facilitated by the structural learning with semantics.

V. EFFECTIVE SEMANTICS-ENHANCED TEMPORAL GRAPH NETWORK

Although semantic aggregation can be easily achieved with the aforementioned frameworks, their utilization of semantics is still coarse. Specifically, the summation semantic aggregator doesn't distinguish the impact of different semantics from the same content on different users, while the concatenation in (15) may be oversimplified to compute proper attention coefficients. Thus, we propose two novel methods to utilize the semantics with high proficiency.

A. User-specific Attention Mechanism for Semantic Aggregation

In order to aggregate multiple semantics fine-grainedly, we can modify the semantic aggregator with an attention mechanism that calculates attention coefficients by analyzing the influence of different genres on the same content. However, it ignores the impact from users, which is also paramount in prediction. Thus, we adopt a UsAttn mechanism to aggregate the multiple semantics, as shown in Fig. 5. For different users,

Algorithm 1 The preference prediction with STGN

Require: Request dataset and pre-trained NLP model;

Ensure: The representations of u_j and i_k , (i.e., E_j^u and E_k^i) and the preference between u_j and i_k .

- 1: Initialize the raw data and the parameters for the whole network and encode contents' semantics information with pre-train NLP model.
- 2: Divide the raw data into several mini batches;
- 3: **for** each batch $(v_{uj}, v_{ik}, e_{ui}, t, S_k) \in$ training dataset **do**
- 4: $\hat{n} \leftarrow$ Sample negatives;
- 5: **if** aggregate S_k by summation **then**
- 6: Aggregate S_k to compute S_k as (13);
- 7: **else**
- 8: Obtain user-specific embedding E_{jk} with (17);
- 9: Aggregate S_k and E_{jk} with (16) and (18);
- 10: **end if**
- 11: Concatenate the message Msg_{jk} with the aggregated semantics in (14);
- 12: Filter and aggregate historical messages in (6) to obtain short-term preference $h_j(\hat{T})$;
- 13: Update long-term preference Mem_j with $h_j(\hat{T})$ in (7);
- 14: Encode the time slot Δ_t with (8) for all nodes;
- 15: **if** semantic positional encoding **then**
- 16: Encode the summarized semantics with (19) and (20);
- 17: **end if**
- 18: Incorporate the encrypted time and semantics features into the updated lone-term preference Mem'_j ;
- 19: Obtain $E_j^u(T_p)$ and $E_k^i(T_p)$ through the TGAT module;
- 20: Predict the preference between users and content with (4);
- 21: Optimize with BCELoss(\cdot);
- 22: **end for**

this mechanism enables the computation of different attention scores for the diverse semantics of the same content and then generates user-specific semantic features. Mathematically, for each content and user, (13) is reformulated as a linear weighted summation of N_s semantics of content i_k , where the weights are calculated by the attention mechanism,

$$S_{jk} = \sigma \left(\sum_{n \in N_s} \alpha_{jn} s_{kn} W_{Vn} \right), \quad (16)$$

$$\alpha_{jn} = \frac{\exp(E_{jk} W_Q \cdot s_{kn} W_{Kn})}{\sum_{m=1}^{N_s} \exp(E_{jk} W_Q \cdot s_{km} W_{Km})},$$

where W_{Kn} , W_Q and W_{Vn} are the trainable parameters, and α_{jn} is the attention coefficient of the n -th semantic message of the content. Especially, E_{jk} is a user-specific embedding, after which we believe the weight calculation will be forced to account for the embeddings of both u_j and i_k . Accordingly, we define it as

$$E_{jk} = \text{LeakyReLU}(W_u E'_{uj} + W_i E'_{ik} + b_{ui}), \quad (17)$$

where W_u , W_i and b_{ui} are the trainable parameters, while E'_{uj} and E'_{ik} ³ are the results generated in the last prediction or the

³For simplicity, we omit the time information \hat{T}' of the last prediction in $E'_{uj}(\hat{T}')$ and $E'_{ik}(\hat{T}')$.

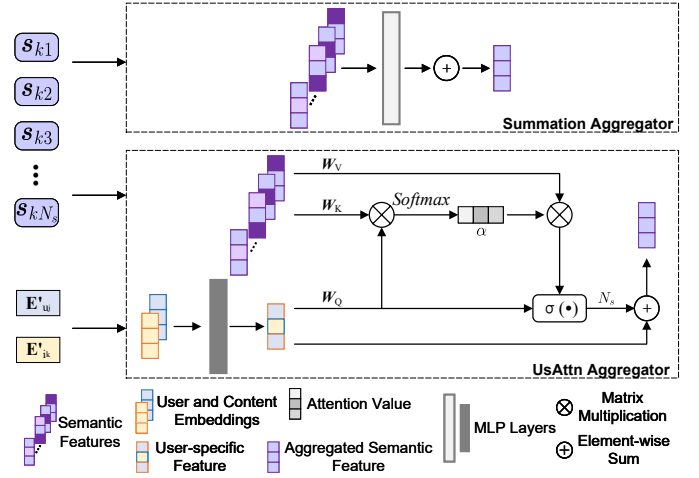


Fig. 5. The illustration of the semantics aggregators. (Upper: Summation Aggregator; Lower: UsAttn Aggregator)

initialization values for the first round prediction of u_j and i_k , respectively.

Moreover, the stacking of multiple DNN layers possibly results in the over-smoothing issue. In this regard, we further leverage the skip-connection in Transformer [21] to avoid this issue and improve the overall performance. Specifically, for each piece of historical message that happened between u_j and i_k , the aggregated semantics is denoted as

$$S_k = N_s \cdot S_{jk} + E_{jk}, \quad (18)$$

which is the desired representation that we use in (14), so as to further optimize M1-STGN or the temporal learning module of M2-STGN.

B. Semantic Positional Encoding for Structural Learning

For different user-content pairs, the proposed UsAttn mechanism allocates different attention weights for content's diverse semantic messages in temporal learning. However, it is hard to generalize this mechanism into the structural learning module. Specifically, the structural learning for i_k is generally conducted by calculating a sub-graph centering around i_k , where all its neighbors are users. In other words, it is elusive for us to determine a specific user before enhancing the structural learning with UsAttn. This dilemma motivates us to find another method to improve semantics utilization in structural learning. Inspired by the positional encoding in Transformer and the time encoding in TGAT, as a Transformer-alike module, it might be also feasible to treat the vertexes' semantic features, generated by (13), as the locators in semantic sphere during the structural learning. Therefore, we ameliorate the model with a specially designed positional encoding function to reinforce the attention effectiveness. To extract useful characteristics from the multi-dimensional semantic position S_k , calculated by (13), we adopt a learnable Fourier features positional encoding function, which is derived in Appendix and can be mathematically formulated as follows,

$$R_k = \frac{1}{\sqrt{D_h}} [\cos W_p \phi_1(S_k) \parallel \sin W_p \phi_1(S_k)]^T, \quad (19)$$

TABLE II
THE VARIANTS OF OUR PROPOSED STGN MODEL, WHERE SUM AND USATTN ARE THE SEMANTIC AGGREGATORS WHILE SPE IS THE EXTRA POSITIONAL ENCODING FOR THE GRAPH ATTENTION MODULE.

	Temporal Learning	Structural Learning
M1-STGN	Sum	-
M2-STGN	Sum	Sum
M1-STGN+U	UsAttn	-
M2-STGN+U	UsAttn	Sum
M2-STGN+SPE	Sum	Sum+SPE
M2-STGN+U+SPE	UsAttn	Sum+SPE

where $\phi_1(\cdot)$ is an MLP layer to enhance the semantic features, and D_h is the dimension of the hidden layer. Notably, the initialized \mathbf{W}_p is drawn from a normal distribution [36]. Furthermore, we also discover that an additional feature enhancement with another MLP is beneficial to the final performance,

$$\mathbf{S}_k \leftarrow \mathbf{W}_p^2 \text{GeLU}(\mathbf{W}_p^1 \mathbf{R}_k), \quad (20)$$

where \mathbf{W}_p^1 and \mathbf{W}_p^2 is the trainable weights, and $\text{GeLU}(\cdot)$ is an activation function that is widely adopted in NLP tasks [31].

After the calculation with (19) and (20), we concatenate the encoded semantic positional embeddings into the input of TGAT layer, as done in (15). Finally, we summarize all variants of our STGN model in Algorithm 1 and highlight their key differences in temporal and structural learning modules in Table II.

VI. EXPERIMENTAL RESULTS AND DISCUSSIONS

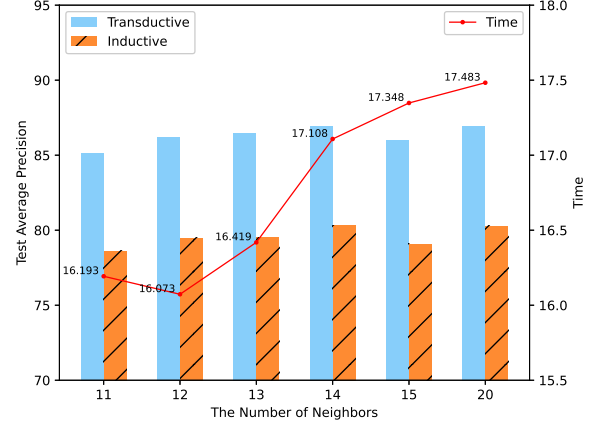
In this section, we present the performance of our proposed models in prediction and caching tasks. We also compare our methods with three state-of-the-art models in processing dynamic graphs, including TGAT [16], DyRep [23], and TGN [25]. Besides, in order to analyze the effectiveness of semantic features, we further adopt some widely-accepted NLP methods to encode the genres, i.e., one-hot, BERT [19], and Glove [20]. Moreover, experiments with respect to the cache hit rate are also conducted to validate the superiority of our model-based caching methods.

A. Experimental Settings

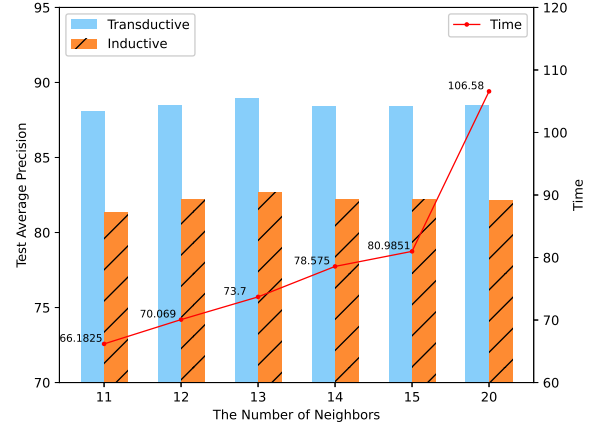
Dataset: In this paper, the experiments are carried out with a public dataset, Netflix⁴, which records a set of user behaviors on Netflix in UK. Notably, there are many insignificant historical messages, such as some users only request once or watch the content for an extremely short period. The burst behavior is hard to be predicted accurately, and it may mislead other predictions as well. Therefore, we select those users who have more than 4 requests and view each requested content for more than 3 minutes as the valid input for the prediction. The dataset we actually adopt includes 86,889 interactions, which involve 11,254 different users and 4,057 pieces of content. The number of interactions is less than the dataset⁵ used in

⁴<https://www.kaggle.com/datasets/vodclickstream/netflix-audience-behaviour-uk-movies>

⁵The dataset used in Ref. [15] involves 5,763 users and 56 contents, which consists of 175,856 interactions.



(a) 1 TGAT Layer



(b) 2 TGAT Layers

Fig. 6. The test average precision and training time of TGN-L with different numbers of aggregating neighbors and TGAT layers.

Ref. [15], while the numbers of users and contents are larger, making the Netflix even much sparser. Afterwards, we perform a 60%-20%-20% chronological split of the dataset for training, validation, and testing, respectively.

Evaluation Tasks and Training Configuration: To verify the effectiveness of our proposed models, we compare our models with several state-of-the-art models, including TGAT [16], DyRep [23], TGN [25] and its variants (i.e., TGN-L, TGN-M and TGN-A). Notably, the receptive field for the graph in GNN is proportional to the number of GNN layers l and the neighbors N_n in each sub-graph. As Ref. [16] suggests, we set $l = 2$ and $N_n = 10$ in TGAT, while $l = 1$ and $N_n = 10$ in TGN. Besides, we also compare our models to the TGN model with larger receptive field, i.e., $l = 1, 2$ and $N_n = 11, 12, 13, 14, 15, 20$.

Furthermore, as for pre-trained NLP models, Glove [20] is conducted by global word-to-word occurrence statistics from a large corpus, while BERT [19] is a neural network model based on 12-layer Transformer. The dimension numbers of their output embeddings are fixed (50 for Glove and 738 for BERT). To reduce the computational cost, we also adopt an MLP to compress the representations of BERT. Besides, Ref. [37] also discovers that the outputs from the 6-th to 10-th layers outperform in semantic tasks. Therefore, we average the embeddings from the 6-th to 10-th layers to investigate

TABLE III

THE TRAINING TIME AND THE PERFORMANCE OF PREDICTING CONTENT REQUESTS IN BOTH TRANSDUCTIVE AND INDUCTIVE TASKS. TGAT AND DYREP ARE TWO STATE-OF-THE-ART DGNN MODELS. TGN-L, TGN-M, AND TGN-A ARE THE CONVENTIONAL TGN MODEL'S VARIANTS WITH DIFFERENT MESSAGE AGGREGATORS. THE BEST RESULTS ARE HIGHLIGHTED IN **BOLD** AND THE SECOND-BEST RESULTS ARE HIGHLIGHTED IN UNDERLINED.

Metric		AUC for Transductive	AP for Transductive	AUC for Inductive	AP for Inductive	Training Time
Baseline	TGAT	75.891	73.426	66.549	65.955	43.711s
	DyRep	84.027	84.096	76.162	77.562	20.116s
	TGN-L	85.299	83.824	77.285	76.995	14.602s
	TGN-M	86.731	86.022	78.953	79.721	90.729s
	TGN-A	90.507	90.691	83.504	84.999	158.163s
M1-STGN	M1-STGN-L	86.386	85.892	79.980	80.439	16.291s
	M1-STGN-M	88.312	88.095	82.043	82.765	91.855s
	M1-STGN-A	91.210	91.337	85.247	86.175	159.239s
M2-STGN	M2-STGN-L	87.383	86.806	81.131	81.182	17.917s
	M2-STGN-M	88.649	88.558	82.805	83.461	91.309s
	M2-STGN-A	91.773	91.953	85.877	87.019	158.754s
M1-STGN+U	M1-STGN-L+U	89.014	88.467	83.096	83.483	16.510s
	M1-STGN-M+U	89.721	89.356	83.585	84.148	92.638s
	M1-STGN-A+U	91.358	91.572	85.327	86.567	158.077s
M2-STGN+U	M2-STGN-L+U	89.749	89.279	84.183	84.387	18.173s
	M2-STGN-M+U	90.107	89.884	84.434	84.868	91.655s
	M2-STGN-A+U	91.846	92.056	86.264	87.279	163.363s
M2-STGN+U+SPE	M2-STGN-L+U+SPE	90.778	90.406	84.582	85.211	19.157s
	M2-STGN-M+U+SPE	90.951	90.641	84.542	85.181	92.235s
	M2-STGN-A+U+SPE	91.240	91.418	85.187	86.430	160.544s

TABLE IV

THE TEST AVERAGE PRECISION RESULTS OF M2-STGN+SPE WITH DIFFERENT NLP METHODS FOR ENCODING THE GENRE INFORMATION.

Semantic model		Transductive	Inductive
One-hot	M2-STGN-L+SPE	87.827	81.581
	M2-STGN-M+SPE	89.730	84.002
	M2-STGN-A+SPE	90.908	85.322
BERT	M2-STGN-L+SPE	87.998	82.300
	M2-STGN-M+SPE	88.972	83.598
	M2-STGN-A+SPE	91.287	86.427
Glove	M2-STGN-L+SPE	88.397	82.447
	M2-STGN-M+SPE	89.392	83.803
	M2-STGN-A+SPE	91.805	86.800

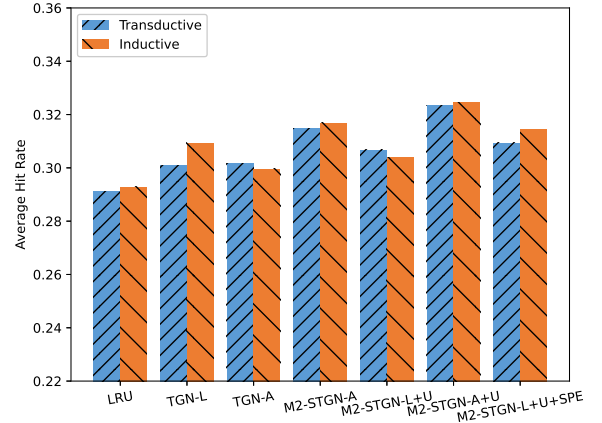


Fig. 7. The average hit rate performance of different algorithms in 24 hours.

the performance.

Moreover, we conduct experiments under two tasks, i.e., transductive task and inductive task. Different from the transductive task, the validation set and test set in an inductive task may contain some vertices that have not been observed by models during the training phase. For both tasks, we adopt the *average precision (AP)* and the *area under the ROC curve (AUC)* as evaluation metrics.

Caching Policy Setting: As depicted in Fig. 3, we configure a multi-layer network architecture. The storage capacity in the device closer to users is typically smaller [33]. Hence, we assume that the *Tier 1* can store 5 contents, while 7 and 8 contents can be cached at *Tier 2* and *Tier 3*, respectively.

As for the content caching task, our target is to predict contents' popularity during 24 hours in the test phase. We assume that the candidate content set \mathcal{I} is known apriori. To make the simulations more practical, we supplement the candidate content set with a noise set, which consists of the

contents that have been requested within a 50-hour duration before the prediction starting time. Besides, the user set \mathcal{U} of each hour is also assumed to be known in our simulation. As for other hyperparameters, we compute the per-hour popularity with $\Delta_P = 1h$ and $\delta_P = 60s$ while the threshold value $p_{thre} = 0.995$.

To verify the superiority of our models in content caching, a comparison between the traditional caching method, LRU, and the prediction results based strategy is also carried out. We deploy TGN-A and its variants, e.g., M2-STGN-A and M2-STGN-A+U, as predictive models. Due to the trade-off between training speed and prediction performance for M2-STGN-L+U and M2-STGN-L+U+SPE, simulations based on them are executed as well. Moreover, testing in the inductive setting, we also conduct extensive ablation studies with M2-STGN-A+U, whose performance in preference prediction

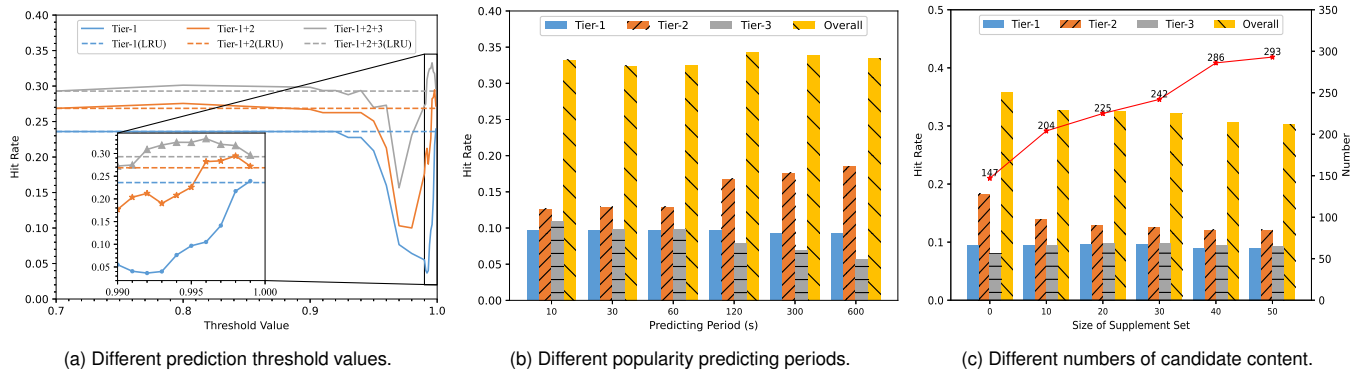


Fig. 8. The hit rate performance in the inductive setting with different hyperparameters for caching.

is the most superior, so as to examine the influence of different hyperparameters (i.e., different sizes of content supplement set and values of δ_P & p_{thre}) on content caching. Notably, we adjust the size of the content supplement set by changing the duration before the starting time.

B. Results Analysis

Table III demonstrates the prediction performance of our proposed TGN models as well as the baseline models. It can be clearly observed that our models are able to yield better results in both transductive task and inductive task, and even the primitive models in M1-STGN outperform the counterparts of TGN. Moreover, the superiority of M1-STGN+U and M2-STGN+U also proves the effectiveness of the UsAttn semantic aggregator. In addition, due to the introduction of SPE, we can also find that the prediction capabilities of most models have been enhanced, especially for the variants of TGN-L and TGN-M. Nevertheless, the results are of little avail when SPE collaborates with a complex model, e.g., M2-STGN-A+U+SPE.

Fig. 6 presents the prediction performance of TGN-L with different sizes of receptive field. As the receptive field enlarges, the performance of TGN-L in both transductive and inductive tasks improves. However, the average training time for obtaining a single model is gradually increasing as well. Compared with the corresponding results in Table III and Fig. 6, we can also discover that most variant models of TGN-L which try to have a deeper insight into the available information through either UsAttn or SPE are superior than methods that enlarge the receptive field (e.g., the stacking of GNN layers or an increase in the number of first-order neighbors) in both prediction performance and training speed. In order to achieve a comparable result to the M2-STGN-L+U+SPE, it takes TGN-L with 2 TGAT layers at least $4\times$ more time. Obviously, our “breadth-first approach” for excavating the inherent relationships is more efficient.

Fig. 7 compares the average hit rate of the caching strategy based on prediction results and LRU for the whole network architecture in both transductive and inductive tasks during 24 hours. It can be observed that relying on our proposed models, the overall caching performance of the prediction-based strategy is always better than LRU. The improvement of prediction accuracy increases the cache hit rate as well.

In particular, the caching strategy based on M2-STGN-A+U surpasses other models, which is in line with the prediction performance. Moreover, considering the trade-off between training speed and the final performance in caching, caching with M2-STGN-L+U+SPE is also promising. Actually, we also conduct simulations for the other two baselines, i.e., TGAT and DyRep, but their poor performance results in too many false positive predictions, failing to distinguish the popularity of contents.

Fig. 8 reveals the hit rate performance in the inductive setting with different hyperparameters for caching. It can be observed in Fig. 8(a) that the caching performance with $p_{thre} < 0.8$ is equivalent to LRU. Since the caching strategy, introduced in Section III-B, decides the prioritization for contents with the same predicted popularity consistent with LRU, such an abnormal phenomenon implies that our model fails to distinguish the popularity of contents when adopting an improper threshold value. However, for a larger threshold, the caching gain from our model becomes more evident, especially when the threshold is close to 1, the strategy relying on our model outperforms the traditional LRU at all tiers. Surprisingly, a more frequent prediction operation does not always lead to an improvement in the hit rate. The simulation results in Fig. 8(b) present that when $\delta_p = 120s$, our model brings the greatest gain to the cache task. On the other hand, Fig. 8(c) shows that the size of candidate content also affects the final caching results. As the number of candidate content gradually increases, it gives rise to a declined overall hit rate, but is still superior to LRU. To sum up, these experiments demonstrate the robustness of the proposed methods.

VII. CONCLUSIONS

In this paper, we have developed an STGN architecture to improve the performance of popularity prediction in a sparse dataset. We have regarded the genres of the contents as semantic information and profiled users’ intentions by attaching the semantics into the conventional TGN. The proposed STGN models have significantly ameliorated the user preference speculation performance. Furthermore, we have devised a UsAttn mechanism for a finer-grained semantic aggregation of diverse genres related to the same content. Meanwhile, an SPE function, targeting at assisting the association analysis in the attention-based graph learning, has been adopted as well.

Due to the superior performance, the caching strategy based on our STGN model also wins a great improvement in cache hit rate under extensive simulations.

Finally, our model provides a paradigm for the fusion of semantics and AI models, where `UsAttn` suggests a novel method to aggregate multiple semantic information fine-grainedly and `SPE` answers the question about how to efficiently incorporate and utilize the aggregated semantic information with AI models. Meanwhile, besides the application in caching, we also believe that it has the potential to be generalized to other network architectures that desire AI models to integrate with semantic analysis, like intent-based network (IBN) [38].

APPENDIX

THE DEDUCTION OF SEMANTIC POSITIONAL ENCODING

As we discussed in Section V-B, we regard the semantic features as a special kind of position in the semantic sphere. However, unlike the context sequence, handled by Transformer [21], the semantic position is a multi-dimension representation. Compared to the cumbersome dimension-independent positional encoding method, we adopt a Fourier kernel-based method to solve this problem.

In our GAT-alike [24] mechanism, the inner-product self-attention belongs to one crucial element in calculating attention coefficients. Consider a continuous position mapping function $\Phi(\cdot)$, for two semantic positions \mathbf{x} and \mathbf{y} , the inner-product between them can be formulated as $\langle \Phi(\mathbf{x}), \Phi(\mathbf{y}) \rangle$. Notably, the relative value, which connotes the distance between two positions, is usually much more important than the absolute position value [16]. Hence, we are more interested in learning a function that is related to the Euclidean distance between two points, i.e., $\sqrt{\|\mathbf{y} - \mathbf{x}\|^2}$. Accordingly, we aim to define a function $\mathcal{K}(\cdot)$, where $\mathcal{K}(\mathbf{x}, \mathbf{y}) = \mathcal{K}(\mathbf{y} - \mathbf{x}) = \langle \Phi(\mathbf{x}), \Phi(\mathbf{y}) \rangle$. It also implies that $\mathcal{K}(\cdot)$ is also a translation-invariant function.

Next, we explain how to find an appropriate $\mathcal{K}(\cdot)$. Beforehand, we would like to present some fundamental lemmas on the Gram matrix, which are introduced in [39],

Lemma 1. *The Gram matrix is symmetric in the case where the real product is real-valued, and the corresponding entries are given by the inner product.*

Lemma 2. *The Gram matrix is positive-semidefinite.*

Therefore, by Lemma (1) and (2), it can be observed that the result of $\mathcal{K}(\mathbf{x}, \mathbf{y})$ can be treated as an element of a Gram matrix and thus \mathcal{K} is also positive semidefinite. Since any positive semidefinite function can be used as a kernel function [39], $\mathcal{K}(\cdot)$ can be taken as a kernel function as well. Moreover, the continuity of the mapping function $\Phi(\cdot)$ implies that the induced kernel $\mathcal{K}(\cdot)$ is continuous. Therefore, \mathcal{K} shall satisfy the assumption of the Bochner's theorem [40].

Lemma 3. *(Bochner's theorem) A continuous, translation-invariant kernel $\mathcal{K}(a, b) = \mathcal{K}(a - b)$ on \mathbb{R}^d is positive definite if and only if $\mathcal{K}(\cdot)$ is the Fourier transform of a non-negative measure.*

Thus, Ref. [36] asserts that $\mathcal{K}(\cdot)$ can be formulated as,

$$\mathcal{K}(a, b) = \mathcal{K}(a - b) = \int_{\mathbb{R}^d} \Pr(\omega) e^{j\omega(a-b)} d\omega = E_{\omega}[\xi(a)\xi(b)^*], \quad (21)$$

where $\xi(b)^*$ is the complex conjugate of $\xi(a)$. $\xi(a) = e^{j\omega a} = \cos(\omega a) + j \sin(\omega a)$ and ω is drawn from $\Pr(\omega)$. Note that the kernel and probability distribution $\Pr(\omega)$ are real, so the imaginary part of $\xi(a)\xi(b)^*$ can be omitted, and (21) can be reformulated as

$$\begin{aligned} \mathcal{K}(a - b) &= E_{\omega}[\cos(\omega(a - b))] \\ &= E_{\omega}[\cos(\omega a) \cos(\omega b) + \sin(\omega a) \sin(\omega b)]. \end{aligned} \quad (22)$$

Therefore, by approximating expectation with the Monte Carlo integral [36], for each dimension x_m and y_m in \mathbf{x} and \mathbf{y} , (22) implies that the inner-product of our kernel can be reformulated as

$$\begin{aligned} \mathcal{K}_m(x_m - y_m) &= \Phi(x_m) \cdot \Phi(y_m) \\ &\approx \frac{1}{D_h} \sum_d (\cos(\omega_d x_m) \cos(\omega_d y_m) + \sin(\omega_d x_m) \sin(\omega_d y_m)) \\ &= \frac{1}{D_h} \cos(\mathbf{w}_m(x_m - y_m)), \end{aligned} \quad (23)$$

where x_m and y_m are the value of m -th dimension in \mathbf{x} and \mathbf{y} , while ω_d is the d -th entry in $\mathbf{w}_m \in \mathcal{R}^{\frac{D_h}{2}}$.

In other words, we can also denote the positional encoding function as $\Phi_m(x) = \frac{1}{\sqrt{D_h}} [\cos \mathbf{w}_m x_m \parallel \sin \mathbf{w}_m x_m]^T$ for each dimension. Then, we can encode the whole vector \mathbf{x} with

$$\Phi(\mathbf{x}) = \frac{1}{\sqrt{D_h}} [\cos \mathbf{W}_p \mathbf{x} \parallel \sin \mathbf{W}_p \mathbf{x}]^T. \quad (24)$$

where $\mathbf{W}_p \in \mathcal{R}^{\frac{D_h}{2} \times D_m}$ is the stacking of \mathbf{w}_m , and D_m is the dimension number of \mathbf{x} .

Furthermore, we pay more attention to the Euclidean distance between the semantic positions, which suggests that $\mathcal{K}(\mathbf{x}, \mathbf{y})$ is the Fourier transform of a normal distribution with respect to ω [36]. Thus, in our algorithm, we initialize entries of \mathbf{W}_p in (19) with a normal distribution while training models.

REFERENCES

- [1] "Cisco annual internet report (2018–2023) white paper," Cisco, 2020. [Online]. Available: <https://www.cisco.com/c/en/us/solutions/collateral/executive-perspectives/annual-internet-report/white-paper-c11-741490.pdf>
- [2] Z. Hajiakhondi Meybodi, A. Mohammadi, E. Rahimian, S. Heidarian, J. Abouei, and K. N. Plataniotis, "TEDGE-Caching: Transformer-based edge caching towards 6G networks," in *Proc. ICC*, Seoul, South Korea, May 2022.
- [3] Y. Shi, K. Yang, T. Jiang, J. Zhang, and K. B. Letaief, "Communication-efficient edge AI: Algorithms and systems," *IEEE Commun. Surv. Tutor.*, vol. 22, no. 4, pp. 2167–2191, 2020.
- [4] "Mobile edge computing (MEC): Technical requirements," ETSI, 2016. [Online]. Available: https://www.etsi.org/deliver/etsi_gs/mec/001_099/002/01.01.01_60/gs_mec002v010101p.pdf
- [5] C. Yang, Y. Yao, Z. Chen, and B. Xia, "Analysis on cache-enabled wireless heterogeneous networks," *IEEE Trans. Wirel. Commun.*, vol. 15, no. 1, pp. 131–145, 2016.
- [6] Q. Chen, W. Wang, W. Chen, F. R. Yu, and Z. Zhang, "Cache-enabled multicast content pushing with structured deep learning," *IEEE J. Sel. Areas Commun.*, vol. 39, no. 7, pp. 2135–2149, 2021.

- [7] O. Serhane, K. Yahyaoui, B. Nour, and H. Mouncla, "A survey of ICN content naming and in-network caching in 5G and beyond networks," *IEEE Internet Things J.*, vol. 8, no. 6, pp. 4081–4104, 2021.
- [8] W. Liu, J. Zhang, Z. Liang, L. Peng, and J. Cai, "Content popularity prediction and caching for ICN: A deep learning approach with SDN," *IEEE Access*, vol. 6, pp. 5075–5089, 2018.
- [9] Z. Zhang and M. Tao, "Deep learning for wireless coded caching with unknown and time-variant content popularity," *IEEE Trans. Wirel. Commun.*, vol. 20, no. 2, pp. 1152–1163, 2021.
- [10] T. Zong, C. Li, Y. Lei, G. Li, H. Cao, and Y. Liu, "Cocktail edge caching: Ride dynamic trends of content popularity with ensemble learning," *IEEE/ACM Trans. Netw.*, vol. 31, no. 1, pp. 208–219, 2023.
- [11] J. Zhou, G. Cui, S. Hu, Z. Zhang, C. Yang, Z. Liu, L. Wang, C. Li, and M. Sun, "Graph neural networks: A review of methods and applications," *AI Open*, vol. 1, pp. 57–81, 2020.
- [12] S. Wu, F. Sun, W. Zhang, X. Xie, and B. Cui, "Graph neural networks in recommender systems: A survey," *ACM Comput. Surv.*, vol. 55, no. 5, pp. 1–37, 2022.
- [13] J. Skarding, B. Gabrys, and K. Musial, "Foundations and modeling of dynamic networks using dynamic graph neural networks: A survey," *IEEE Access*, vol. 9, pp. 79 143–79 168, May 2021.
- [14] Y. Fu, L. Salaün, X. Yang, W. Wen, and T. Q. S. Quek, "Caching efficiency maximization for device-to-device communication networks: A recommend to cache approach," *IEEE Trans. Wirel. Commun.*, vol. 20, no. 10, pp. 6580–6594, 2021.
- [15] J. Zhu, R. Li, G. Ding, C. Wang, J. Wu, Z. Zhao, and H. Zhang, "AoI-based temporal attention graph neural network for popularity prediction and content caching," *IEEE Trans. on Cogn. Commun. Netw.*, 2022, Early Access.
- [16] D. Xu, C. Ruan, E. Korpeoglu, S. Kumar, and K. Achan, "Inductive representation learning on temporal graphs," in *Proc. ICLR*, Virtual Edition, Apr./May 2020.
- [17] J. Liang, D. Zhu, H. Liu, H. Ping, T. Li, H. Zhang, L. Geng, and Y. Liu, "Multi-head attention based popularity prediction caching in social content-centric networking with mobile edge computing," *IEEE Commun. Lett.*, vol. 25, no. 2, pp. 508–512, 2021.
- [18] Y. Liu, S. Yang, Y. Xu, C. Miao, M. Wu, and J. Zhang, "Contextualized graph attention network for recommendation with item knowledge graph," *IEEE Trans. Knowl. Data Eng.*, vol. 35, no. 1, pp. 181–195, 2023.
- [19] J. Devlin, M. Chang, K. Lee, and K. Toutanova, "BERT: pre-training of deep bidirectional transformers for language understanding," in *Proc. NAACL-HLT*, Minneapolis, Minnesota, USA, Jun. 2019.
- [20] J. Pennington, R. Socher, and C. D. Manning, "Glove: Global vectors for word representation," in *Proc. EMNLP*, Doha, Qatar, Oct. 2014.
- [21] A. Vaswani, N. Shazeer, N. Parmar, J. Uszkoreit, L. Jones, A. N. Gomez, L. Kaiser, and I. Polosukhin, "Attention is all you need," in *Proc. NeurIPS*, Long Beach, CA, USA, Dec. 2017.
- [22] D. Lee, J. Choi, J.-H. Kim, S. Noh, S. L. Min, Y. Cho, and C. S. Kim, "LRFU: A spectrum of policies that subsumes the least recently used and least frequently used policies," *IEEE Trans. Comput.*, vol. 50, no. 12, pp. 1352–1361, 2001.
- [23] R. Trivedi, M. Farajtabar, P. Biswal, and H. Zha, "DyRep: Learning representations over dynamic graphs," in *Proc. ICLR*, New Orleans, LA, USA, May 2019.
- [24] P. Veličković, G. Cucurull, A. Casanova, A. Romero, P. Lio, and Y. Bengio, "Graph attention networks," in *Proc. ICLR*, Vancouver, BC, Canada, Apr./May 2018.
- [25] E. Rossi, B. Chamberlain, F. Frasca, D. Eynard, F. Monti, and M. Bronstein, "Temporal graph networks for deep learning on dynamic graphs," in *Proc. ICML 2020 Workshop on Graph Representation Learning*, Virtual Edition, Jul. 2020.
- [26] H. Wang, F. Zhang, J. Wang, M. Zhao, W. Li, X. Xie, and M. Guo, "Ripplenet: Propagating user preferences on the knowledge graph for recommender systems," in *Proc. CIKM*, Torino, Italy, Oct. 2018.
- [27] Y. Li, X. Guo, W. Lin, M. Zhong, Q. Li, Z. Liu, W. Zhong, and Z. Zhu, "Learning dynamic user interest sequence in knowledge graphs for click-through rate prediction," *IEEE Trans. Knowl. Data Eng.*, vol. 35, no. 1, pp. 647–657, 2023.
- [28] X. Wang, D. Wang, C. Xu, X. He, Y. Cao, and T.-S. Chua, "Explainable reasoning over knowledge graphs for recommendation," in *Proc. AAAI*, Honolulu, Hawaii, USA, Jan./Feb. 2019.
- [29] H. Mezni, D. Benslimane, and L. Bellatreche, "Context-aware service recommendation based on knowledge graph embedding," *IEEE Trans. Knowl. Data Eng.*, vol. 34, no. 11, pp. 5225–5238, 2022.
- [30] N. Kitaev, L. Kaiser, and A. Levskaya, "Reformer: The efficient transformer," in *Proc. ICLR*, Virtual Edition, Apr./May 2020.
- [31] Y. Li, S. Si, G. Li, C.-J. Hsieh, and S. Bengio, "Learnable fourier features for multi-dimensional spatial positional encoding," in *Proc. NeurIPS*, Virtual Edition, Dec. 2021.
- [32] N. J. Parmar, A. Vaswani, J. Uszkoreit, L. Kaiser, N. Shazeer, A. Ku, and D. Tran, "Image transformer," in *Proc. ICML*, Stockholm, Sweden, Jul. 2018.
- [33] O. Ayoub, F. Musumeci, M. Tornatore, and A. Pattavina, "Energy-efficient video-on-demand content caching and distribution in metro area networks," *IEEE Trans. Green Commun. Netw.*, vol. 3, no. 1, pp. 159–169, Mar. 2019.
- [34] B. Chen and C. Yang, "Caching policy for cache-enabled d2d communications by learning user preference," *IEEE Trans. Commun.*, vol. 66, no. 12, pp. 6586–6601, 2018.
- [35] J. Chung, C. Gulcehre, K. Cho, and Y. Bengio, "Empirical evaluation of gated recurrent neural networks on sequence modeling," in *Proc. NeurIPS*, Montreal, QC, Canada, Dec 2014.
- [36] A. Rahimi and B. Recht, "Random features for large-scale kernel machines," in *Proc. NeurIPS*, Vancouver, BC, Canada, Dec. 2007.
- [37] G. Jawahar, B. Sagot, and D. Seddah, "What does BERT learn about the structure of language?" in *Proc. ACL*, Florence, Italy, Jul./Aug. 2019.
- [38] A. Leivadreas and M. Falkner, "A survey on Intent-Based Networking," *IEEE Commun. Surveys Tuts.*, vol. 25, no. 1, pp. 625–655, 2023.
- [39] G. R. Lanckriet, N. Cristianini, P. Bartlett, L. E. Ghaoui, and M. I. Jordan, "Learning the kernel matrix with semidefinite programming," *J. Mach. Learn. Res.*, vol. 5, no. Jan, pp. 27–72, 2004.
- [40] W. Rudin, *Fourier analysis on groups*. Courier Dover Publications, 2017.